

Aerosol optical depth variability in the northeastern Arabian sea during winter monsoon: a Study using *in-situ* and satellite measurements

Prakash Chauhan, Nivedita Sanwani & R R Navalgund

Space Applications Center, Indian Space Research Organization, Ahmedabad-380 015, India

Received 2 November 2007; revised 19 January 2009

Presents study consists the results of the Sun photometer measurements of aerosol optical depth (AOD) over the northern Arabian Sea during December 4-17, 2004 along with OCEANSAT-1 Ocean Colour Monitor (OCM) data derived AOD estimates. *In-situ* AOD ranged between 0.15-0.38 at 500-nm wavelength (with a mean of 0.274). Relatively higher values of angstrom exponent (mean=1.8) were observed during the cruise period, indicating presence of smaller particles, which seem to have advected from Indian subcontinent and associated with favorable wind conditions as shown by wind vector data from Quikscat scatterometer. The Spatial distribution of the AOD over the study area was derived using OCEANSAT-1 OCM satellite data. OCM derived AOD images showed plumes of high aerosol optical depth originating near the coastal regions and dispersing over oceanic regions. The satellite data derived AOD values were also compared with *in-situ* measurements. OCM derived AODs matched well with *in-situ* measurements having an RMSE of sixteen percent for seven match-up points.

[**Keywords:** Aerosol, Earth, Angstrom, Scatter, Meteorology]

Introduction

During the last century, Earth's surface temperature has been reported to have increased by $\sim 0.6^{\circ}\text{C}^1$. This rapid temperature change has been attributed to a balance between absorption of incoming solar radiation and emission of thermal radiation from the Earth system. The aerosols, though minute particles in the Earth system, play a major role in this process. It play a major role in dampening the surface temperature rise. The role of the aerosols in influencing the net radiation budget of the earth has been a subject of critical extensive study by many researchers²⁻³. The aerosols also affect cloud microphysics and those with land origin possibly reduce Indian summer monsoon rainfall⁴. Dynamic and diverse nature of the aerosols varies according to different locations. The aerosols originating due to desert dust, rural atmospheric situations, urban pollutants and marine areas have wide variations and display specific characteristics. Their variability over time and space definitely merits continuous monitoring and characterization in respect of their spectral properties. The oceans, which cover over 70% of the earth's surface, are the largest source of natural aerosols. Marine aerosols are hygroscopic and are crucial in cloud formation around the marine boundary layer.

During the months of December–February, northeasterly winds over the Indian subcontinent carry aerosols from the land towards the oceanic atmosphere⁵. These months therefore, become most ideal period to study the effect of continental aerosols and their dispersal in the oceanic atmosphere. A large number of observations have been recorded over the Arabian Sea during the various campaigns e.g. INDOEX, Aerosol Characterization Experiment (ACE) etc. to characterize aerosol variability, optical properties and chemical composition. Measurements and chemical analysis during the INDOEX have shown the Indo-Asian haze spreading in the north Indian Ocean consisting of inorganic and carbonaceous particles, including black carbon clusters, fly ash and mineral dust⁶.

Most of these *in-situ* data campaigns for aerosol characterization have provided significant information on spectral variability, aerosol type, particle size etc., however, *in-situ* data do not provide information on the spatial distribution and transport process of aerosols. Routine monitoring of aerosol events and their subsequent dispersal pattern are important in order to understand their role in climatic process. The satellite sensors provide platform for making observations covering large area as also their short-term and frequent repeatability⁷. Ocean-colour sensors

e.g. CZCS, SeaWiFS, MODIS, POLDER, OCEANSAT-1 OCM have been used to study aerosols, apart from being used to study ocean-colour^{8,9}. Most of the ocean-colour sensors are equipped with a few additional near infrared (NIR) bands ($\lambda > 700\text{nm}$), which are helpful in providing vital information on atmospheric aerosols due to strong absorption by water in NIR wavelengths. OCEANSAT-1 Ocean Colour Monitor (OCM) is one such satellite providing ocean-colour measurements since June 1999 around the sea adjoining the Indian subcontinent. Das *et al.* (2003)^{8,10} have shown the use of OCM data for the estimation of aerosol optical depth (AOD) and its spatial and temporal behavior over the Indian Ocean region.

The present work is an attempt to investigate the temporal, spectral and spatial variations of marine AOD over the northeastern Arabian Sea. It is based on the *in-situ* measurements taken on-board a research vessel Sagar Kanya and OCEANSAT-1 OCM sensor derived AODs during the first fortnight of December 2004 in the north-eastern Arabian Sea. The satellite derived AOD values have been compared with the *in-situ* measurements and aerosol transport from Indian land mass is also studied along with the Quikscat scatterometer derived wind vector data.

Materials and Methods

The *in-situ* aerosol optical depth data were collected on-board *ORV Sagar Kanya*, cruise number SK-214, during 4th December 2004 to 17th December 2004. Fig. 1 shows the ship cruise track and the sampling stations covered. Starting from Goa, the ship moved northwestwards into the ocean away from the coast and reached the northernmost point on 14 December 2004. Then it returned to Goa on a track closer to the coast. The numbers marked in Fig.1 on the cruise track represent the dates of AOD observations. The cruise area was confined within the latitudes 15.14 -16.98° N and longitudes 73.57-72.42° E, covering open ocean and coastal regions around northeastern Arabian Sea.

The aerosol optical (AOD) measurements were made using a multispectral Microtops Sun-Photometer (Solar Light Co., USA). It measured AOD at five different wavelengths centered at 380, 440, 500, 675 and 870-nm, from the instantaneous solar flux measurements using its internal calibration. The onboard measurements were carried out following the standard AOD measurement protocols for ship-borne

surveys¹¹. In general, most of the observations were cloud free and a good quality dataset could be obtained. During cruise the Sun photometer was operated from 0900hrs to 1600hrs at half-hourly interval. AOD measurements were made from the ship deck when the sky was cloud free or when clouds were far away from the solar disk. Simultaneous meteorological observations like wind speed and relative humidity were recorded by an automatic weather station and the atmospheric pressure were measured with an on-board aneroid barometer.

OCEANSAT-1 OCM satellite data was obtained corresponding to the *in-situ* data collected in the Arabian Sea during 4th December 2004 to 16th December 2004, having path 9 and rows numbers 13 and 14 covering the study area for every alternate day, since OCM has two-day repetivity. Total number of 7 scenes for 14 days (Dec. 4-16, 2004) were processed to obtain OCM derived AOD distribution over the study area. OCM data records reflected radiation from earth's surface in eight spectral bands ranging within 412-865nm wavelengths. The NIR wavelength band of 865-nm has been used for the estimation of aerosol optical depth over the oceanic surfaces.

Daily near surface wind vector data corresponding to the OCM scenes for the cruise period was obtained from Quikscat Scatterometer of NASA (data was

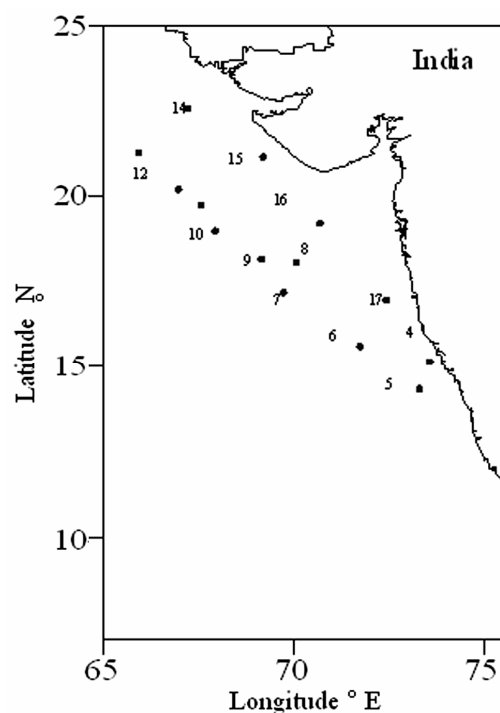


Fig. 1— Cruise Track for SK-214 data collection campaign

downloaded from PODAAC web site <http://poet.jpl.nasa.gov>). The wind velocity ranged from 2 to 10m/s and the direction of wind being from Indian landmass towards the ocean.

Estimation of AOD from OCEANSAT-1 OCM data

Space borne ocean colour remote sensor detected top of the atmosphere (TOA) radiance are contaminated by solar radiation backscattered by the atmospheric air molecules and aerosols. This radiance is called the atmospheric path radiance. In order to correct for atmospheric interference in the remote sensing of oceanic constituents, ocean colour sensors are generally equipped with additional channels in wavelengths above ~700 nm. These NIR bands of ocean colour sensors also provide information on atmospheric aerosols. Das *et al.* (2002)¹² has developed a methodology to estimate aerosol optical depth using single band (765-nm) of OCM data. In the present study the method adopted by Das *et al.* (2002)¹² has been used, however, we have selected 865-nm band of OCM data for AOD inversion. Since 765-nm band of OCM data has significant contribution from oxygen (O₂A) absorption and it has been shown by Ding and Gordon (1995)¹³ that this O₂A absorption reduces top of the atmosphere (TOA) signal in this band by ~10-15%. The use of 765-nm band of OCM data may lead to underestimation of estimated AOD values. Keeping this in view, the method adopted by Das *et al.* (2002)¹² was modified for OCM band 865-nm.

The basis of AOD estimation using 865-nm band of OCM data lies in the fact that for NIR bands ($\lambda > 700\text{nm}$) ocean surface acts as a dark background because of the high absorption by water. The sensor-detected radiances can be assumed to be is just the sum of the Rayleigh and Aerosol path radiance produced by the scattering of light by air molecules and aerosols. In the present study single scattering assumption has been considered and multiple scattering effects have been neglected due to relatively narrow viewing geometry of OCM sensor (i.e. $\pm 45^\circ$). According to Doerffer (1992)¹⁴ radiances detected by a space borne sensor at top of atmosphere (TOA) at wavelength $\lambda > 700\text{nm}$ can be split into

$$L_t = L_a + L_r \quad \dots (1)$$

where, L_t represents the Sensor detected radiance; $L_a = (F_o \cdot \omega_{oa} \cdot \tau_a \cdot P_a(\vartheta)) / (4\pi \cos \vartheta_v)$ represents the Aerosol path radiance; $L_r = (F_o \cdot \omega_{or} \cdot \tau_r \cdot P_r(\vartheta)) / (4\pi \cos \vartheta_v)$

represents the Rayleigh path radiance; F_o is the extraterrestrial solar flux; ϑ_v represents the Satellite viewing angle; ω_{oa} represents the Aerosol single scattering albedo; ω_{or} represents the Rayleigh single scattering albedo (~1.0); τ_a represents the Aerosol optical depth; τ_r represents the Rayleigh optical depth; $P_a(\vartheta)$ represents the function related to Aerosol scattering Phase function; $P_r(\vartheta)$ represents the function related to Rayleigh scattering Phase function.

The relationship between $P_a(\vartheta)$ and $P_r(\vartheta)$ which are related to the Aerosol/Rayleigh scattering Phase function as established by Doerffer (1992)¹⁴ is given as

$$P_a(\vartheta) = P_a(\vartheta^-) + [R(\vartheta_v) + R(\vartheta_s)] P_a(\vartheta^+) \quad \dots (2)$$

where, $R(\vartheta_v)$ stands for Fresnel reflectance of the water surface along (ϑ_v) satellite viewing angle; $R(\vartheta_s)$ stands for Fresnel reflectance of the water surface along (ϑ_s) solar zenith angle; ϑ^\pm represents the Forward (+)/Backward (-) scattering angle.

Das *et al.* (2002)¹² have shown that the aerosol phase function for marine aerosols can be approximated by the two-term Henyey - Greenstein phase function of the following form

$$P_a(\vartheta^\pm) = \alpha \cdot f(\vartheta^\pm, g_1) + (1 - \alpha) \cdot f(\vartheta^\pm, g_2) \quad \dots (3)$$

$$f(\vartheta^\pm, g) = (1 - g^2) / [(1 + g^2 - 2g \cos \vartheta^\pm)^{3/2}] \quad \dots (4)$$

with $\alpha = 0.985$, $g_1 = 0.8$, $g_2 = 0.5$ for marine aerosols¹⁴. Since aerosol properties vary in space and time, hence for a satellite overpass it is not practical to use realistic phase functions of marine aerosols, therefore a two-term HG phase function has been used in this study. Assuming $\omega_{oa} \approx 1.0$ for marine aerosols, the aerosol optical depth (AOD) from the sensor-detected radiance at 865nm wavelength has been inverted as

$$\tau_a = [(L_t - L_r) \cdot 4\pi \cdot \cos \vartheta_v] / [F_o \cdot \omega_{oa} \cdot P_a(\vartheta)] \quad \dots (5)$$

Using equation (5) OCM data for the path 9 and row 13 and 14 was processed for December 4-16, 2004 period to generate spatial distribution of aerosol optical depth over the Arabian Sea.

Results and Discussion

The spectral variations of AODs at five wavelengths for the entire cruise are shown in Figure 2. The daily average AOD values at 500 nm wavelength for 14 days of observations were mostly in the range of ~0.1 to 0.4. Maximum AOD value of 0.38 at 500nm was observed on December 16, 2004

with overall mean value of 0.27 for all the observations during the cruise duration. We have divided the measurements, in the near coast and far coast regions based on the distance from coast. This division is arbitrary, but sufficient to illustrate the differences between the aerosols spectral properties close to and far from land. The AOD data collected during December 6-13, 2004 represent mainly oceanic environment and remaining data set was considered to represent the coastal atmosphere. Corresponding averages at all five wavelengths are given in Table 1. It is noted that τ_a at 500nm was 0.24 over the regions away from the coast, and when the ship approached the coastal waters the mean $\tau_a(500 \text{ nm})$ value has increased to 0.30. Overall it can be seen that the values of τ_a obtained from cruise SK-214, decreased as the ship moved away from the coast in to the deep ocean and increased as the ship approached the coast again. This seems to be associated with westerly winds blowing from the Arabian continent towards the Arabian Sea during November – April period causes advection of Arabian air mass over to the northern parts of Arabian Sea¹⁵. Fig. 2, shows lesser spectral variations in AOD values in the regions far away from coast as compared to that of near coast stations clearly giving information about the particle size distribution. The particle size of marine aerosol is also large in comparison to that in the continental aerosols. The far-coast regions are dominated by Mie scattering, whereas Rayleigh scattering affects the near-coast regions. These observations appear to be

realistic and are as expected since the micro-physical processes, such as gravitational settling of large aerosol; coagulation, condensation and cloud cycling of the small aerosols combined with absence of significant sources over the ocean, lead to a continuously decreasing aerosol loading as one moves to farther oceanic regions.

Spectral measurements of the AOD also provide indirectly the information on the particle size distribution in the total atmospheric column. The inverse power law for spectral variation of AODs is given as

$$\tau = \beta \lambda^{-\alpha} \quad \dots (7)$$

where, α , β and λ represents the Angstrom exponent, the turbidity factor and the wavelength used respectively. The value of α depends on the proportion of the concentration of large to small aerosol particles and is related in such a manner that higher value of α indicates dominance of smaller aerosol particles. β represents the total aerosol loading in the atmosphere and as such a higher value of β gives an indication of poor visibility due to higher turbidity level. A relatively large mean value of α was obtained over the coastal (~1.12) stations as compared to the open ocean (~1.05) stations (*see table 1*). Relatively large values of α and β found in the coastal water regions indicate presence of relatively higher concentration of smaller size particles as compared to the measurements over the open ocean waters. These values of Angstrom exponent can also be attributed to the high aerosol loading close to the coast, arising mainly from the anthropogenic activities over the coastal regions. The western coastal regions of India off Maharashtra and Gujarat shores are highly industrialized and urbanized and the aerosols resulting from these activities dominate the near coastal regions. These observations also can be explained by the predominant wind direction during the month of December. The wind direction is westerly and wind blows from the Indian landmass over to the Arabian Sea during November–April period, which causes advection of continental aerosols over the northeastern parts of Arabian Sea. Fig. 3(b) shows the

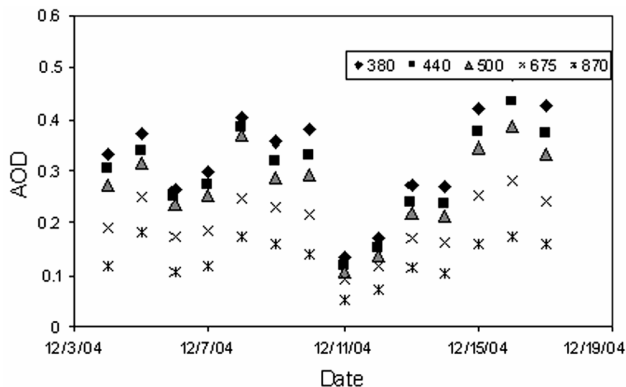


Fig. 2— Spectral variations of the aerosol optical depth (AOD) in different bands at 1030 hrs for the cruise dates.

Table 1—Statistics of the AOD and angstrom exponents observed during the cruise period

Location	Aerosol Optical Depth at λ (nm)					Angstrom Exponent α
	380	440	500	675	870	
Cruise region	0.33±0.04	0.29±0.03	0.27±0.03	0.20±0.02	0.13±0.01	1.08±0.03
Coastal water	0.37±0.05	0.33±0.05	0.30±0.04	0.23±0.13	0.14±0.02	1.12±0.06
Open water	0.30±0.05	0.27±0.05	0.24±0.04	0.19±0.10	0.12±0.02	1.05±0.03

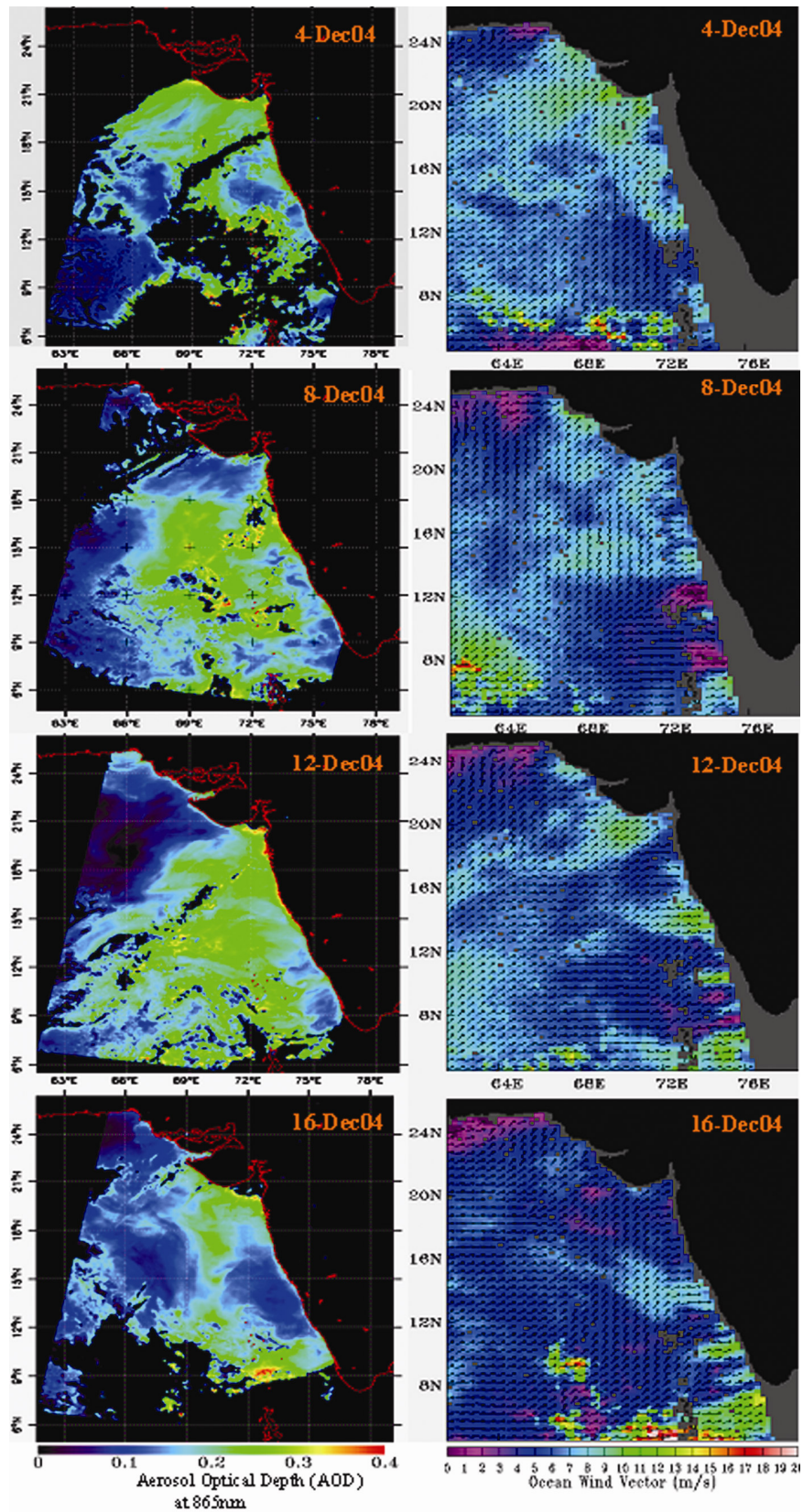


Fig. 3— (a) OCEANSAT-1 OCM derived aerosol optical depth for the period of Dec 4-16, 2004 and (b) corresponding wind vectors derived from Quikscat scatterometer data.

wind vector as derived through Quikscat scatterometer over the Arabian Sea during December 2004.

OCEANSAT-1 OCM data for cruise duration of December 4-16, 2004 for pass number 9 and rows 13 and 14 was processed for the AOD estimation at 865-nm wavelength using the methodology described in the section 3.0. The AOD images generated for pass 9 row 13 and pass 9 row 14 were mosaiced to generated AOD images covering eastern part of the Arabian Sea adjoining the entire west coast of India. Fig. 3(a) shows the OCEANSAT-1 OCM derived AOD images for December 4, 8, 12 and 16, 2004 along with the Quikscat scatterometer derived wind vector data (Fig. 3(b)). OCM derived AOD images clearly show advection of aerosol plumes from the Indian continent over the Arabain Sea waters.

A comparative analysis of the OCM derived AOD at 865nm was done with *in-situ* measured AOD values using the hand held sun-photometer. A good correlation between OCM derived and *in-situ* measured AODs was obtained for the cruise duration. Fig. 4 shows the relationship between OCM derived and *in-situ* measured AOD values at 865-nm wavelength for seven match-up locations. Only seven math-up locations could be achieved during the cruise duration of December 4-17, 2004, due to two-day repetivity of OCM sensor. OCM derived and *in-situ* measured AOD values showed a correlation coefficient, r^2 of 0.89 and an RMS error of sixteen percent.

Conclusions

In-situ measurements of the Aerosol Optical Depth (AOD) were made in the Arabian Sea during

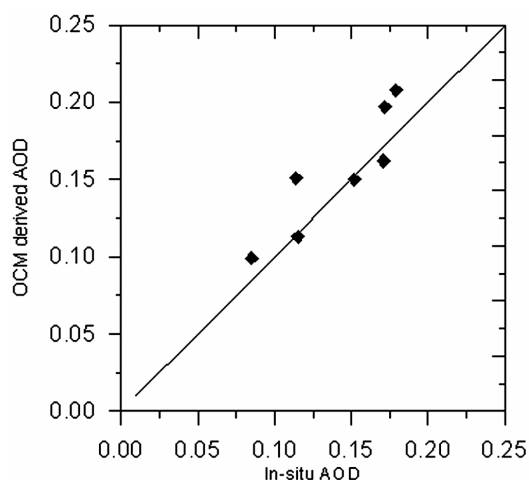


Fig. 4— Comparison of Microtops Sun photometer derived AODs with OCEANSAT-1 OCM derived AODs at 12 00 hrs (IST) during the cruise

December 4-17, 2004 on-board ORV Sagar Kanya using a hand-held sun photometer. During the ship-cruise period Aerosol Optical Depth (AOD) was also estimated using the OCEANSAT-1 OCM sensor. Following conclusions are drawn from this study. The AOD values decreased as the ship moved away from the coast to the open oceanic regions. The optical depth gradually decreased with distance from the coast. Mean AOD value at 500 nm was found to be 0.25 over the regions away from the coast and was found to be 0.31 near the coast. The AOD at 500 nm averaged at 0.274 for the entire cruise. The average values of Angstrom exponent (α) and turbidity factor (β) for near the coast and far coastal regions were 1.80 and 0.10 respectively. Measurements show relatively higher concentration of smaller size particles over coastal regions as compared to that over the open ocean waters. These continental aerosols over near coast regions are dominated by Rayleigh scattering and are, therefore, responsible for maximum scattering of incoming solar radiation whereas marine aerosols over far coast regions are dominated by Mie scattering. Spatial distribution of aerosols could be obtained using the OCEANSAT-1 OCM derived AOD images. These images show a very high-resolution view of aerosol structures and their advection behavior. OCM derived AOD images were also validated with *in-situ* measured AOD and a good correlation with $r^2=0.89$ and RMS=16% was obtained between the two measurements. Quikscat scatterometer derived wind vector images also provided some indication of advection of continental aerosols over the marine environment.

References

- 1 Intergovernmental Panel of Climate Change. Climate Change 2001 – The Scientific Basis (contribution of working group 1 to the Third Assessment Report of the Intergovernmental Panel on Climate Change) (Cambridge Univ. Press, Cambridge, 2001).
- 2 Coakley J A, Cess R D & Yurevich F B, The effect of tropospheric aerosols on the earth’s radiation budget: A parameterisation for climate models, *J. Atmos. Sci.*, 40 (1983) 116–138.
- 3 Satheesh S K, Krishnamoorthy K & Das I, Aerosol optical depths over the Bay of Bengal, Arabian Sea & Indian Ocean, *Current Science*, 81 (2001) 425–435
- 4 Patra P K, Behera S K, Herman J R, Maksyutov S, Akimoto H, and Yamagata T, Indian summer monsoon rainfall: Interplay of coupled dynamics, radiation balance and cloud microphysics, *Atmos. Chem. Phys.*, 5 (2005) 2181–2188.
- 5 Das I & Mohan M, Detection of marine aerosols using ocean colour sensors, *Mausam*, 54 (2003) 327–334.

- 6 Satheesh S K & Krishna Moorthy K, Aerosol characteristics over coastal regions of the Arabian Sea. *Tellus*, B49 (1997), 417–428.
- 7 Ramanathan V *et al.*, Indian Ocean Experiment: An integrated analysis of the climate forcing and effects of the great Indo-Asian haze. *J. Geophys. Res. D*, 106 (2001) 28,371–28,398.
- 8 Das I & Mohan M, Detection of marine aerosols using ocean colour sensors, *Mausam*, 54 (2003) 327–334.
- 9 Kaufman Y J, Tanre D, Gordon H R, Nakajima T, Lenoble J, Frouin R, Grassl H, Herman B M, King M D & Teillet P M, Passive remote sensing of tropospheric aerosol and atmospheric correction for the aerosol effect, *J. Geophys. Res.*, 16 (1997) 815 – 830.
- 10 Das I, Shukla A K & Mohan M, Aerosols in northeast Arabian Sea during the Indian winter monsoon: a study using sunphotometer measurements, *Current Science*, 86 (2004) 1304-1308.
- 11 Frouin R, Holben B, Miller M, Pietras C, Kirk K D, Fargion G S, Porter J, Voss K, Sun and sky radiance measurements and data analysis protocols. In: Muller J F Fargion GS McClain C R (Eds). Ocean Optics protocols for satellite ocean colour sensor validation, revision 4, Radiometric measurements and data analysis protocol., NASA TM-2003-211621/Rev-4-Vol-111, NASA Goddard Space flight Centre, Green belt, MD, (2003), pp. 60-69.
- 12 Das I, Mohan M, & Krisnamoorthy K, Detection of marine aerosols with IRS-P4 Ocean Colour Monitor, *Proc. Indian Acad. Sci. (Earth & Planet Sci.)*, 111 (2002), 425-435.
- 13 Ding K & Gordon M, Analysis of the influence of O₂A-band absorption on atmospheric correction of ocean-color imagery, *Applied Optics*, 34 (1995) 2068-2080.
- 14 Doerffer R, *Imaging spectroscopy for detection of chlorophyll and suspended matter, in Imaging spectroscopy: Fundamentals and Prospective Applications*, edited by F. Toselli and Bodechtel, (Kluwer Academic Publishers, Dordrecht/Boston/London) 1992 pp 215-255.
- 15 Satheesh S K & Ramanathan V, Large differences in tropical forcing at the top of the atmosphere and Earth's surface, *Nature*, 405 (2000), 60 - 63.